

Rafał Skupio

*Oil and Gas Institute – National Research Institute*

## Accuracy assessment of the determination of radioactive elements concentration on shale cores

Precise knowledge of the concentration of radioactive elements can be applied for lithological identification of the rocks, particularly for identifying shale layers. Those rocks are characterised by a high natural radioactivity, due to the presence of clay minerals as well as organic matter. The presence of the organic matter significantly increases the concentration of uranium. It is therefore a quick way of identifying the intervals of hydrocarbon potential. In the present study, the accuracy of establishing the concentration of radioactive elements: potassium ( $^{40}\text{K}$ ) – 1.46 MeV, uranium ( $^{238}\text{U}$ ) – 1.76 MeV and thorium ( $^{232}\text{Th}$ ) – 2.62 MeV was examined for shale formation. The research was conducted with the use of a 9-window decomposition method of gamma radiation spectra. The spectra were registered with a spectrometer – Gamma Logger (Core Lab WSGL-300-T), adjusted to the measurement of the natural radioactivity of core samples. The current application of the gamma spectrometer consisted mainly of establishing the total radioactivity. It is due to the low efficiency of the detection process of the 3-window method, implemented in the software of the device. The GL spectrometer is equipped with a detection system of a high energy resolution (about 7% for  $^{137}\text{Cs}$ ), which allows for the application of the 9-window method, providing additional information from the low-energy part of the spectrum, below 1.3 MeV. This method improves the accuracy of measurements of the concentration of radioactive elements, due to both the significantly higher count of the detector readings, which lessens the influence of statistical fluctuations, as well as the additional energy lines for uranium and thorium.

Key words: gamma radiation, spectral gamma ray decomposition, gamma logging, natural radioactivity, shale rocks.

### Ocena dokładności wyznaczania koncentracji pierwiastków promieniotwórczych na rdzeniach skał łupkowych

Dokładna znajomość koncentracji pierwiastków promieniotwórczych może być wykorzystywana w identyfikacji litologicznej badanego ośrodka skalnego, zwłaszcza w poszukiwaniu/wyznaczaniu warstw łupkowych. Skały te charakteryzują się wysoką naturalną promieniotwórczością wynikającą zarówno z obecności minerałów ilastych, jak i substancji organicznej. Występowanie substancji organicznej znacznie zwiększa koncentrację uranu. Jest to zatem szybki sposób na identyfikację interwałów o potencjale węglowodorowym. Ocena dokładności wyznaczania koncentracji pierwiastków promieniotwórczych: potasu ( $^{40}\text{K}$ ) – 1,46 MeV, uranu ( $^{238}\text{U}$ ) – 1,76 MeV i toru ( $^{232}\text{Th}$ ) – 2,62 MeV, została wykonana dla skał formacji łupkowej. Badania przeprowadzono z wykorzystaniem 9-oknowej metody dekompozycji widm promieniowania gamma. Widma były zarejestrowane przy pomocy spektrometru – Gamma Logger WSGL-300-T, przystosowanego do pomiarów naturalnej promieniotwórczości rdzeni wiertniczych. Dotychczasowe wykorzystanie spektrometru gamma polegało głównie na wyznaczaniu całkowitej promieniotwórczości „total”. Wynika to z niskiej wydajności detekcji w metodzie 3-oknowej, która jest zaimplementowana w oprogramowaniu urządzenia. Spektrometr GL wyposażony jest w układ detekcyjny o wysokiej rozdzielczości energetycznej (około 7% dla  $^{137}\text{Cs}$ ), co pozwala zastosować metodę 9-oknową dostarczającą dodatkową informację z niskoenergetycznej części widma, poniżej 1,3 MeV. Metoda ta pozwala na poprawę dokładności pomiarów koncentracji pierwiastków promieniotwórczych, zarówno ze względu na znacząco większą ilość zliczeń detektora, co obniża wpływ fluktuacji statystycznych, jak i ze względu na dodatkowe linie energetyczne dla uranu i toru.

Słowa kluczowe: promieniowanie gamma, dekompozycja widm, profilowanie gamma, promieniotwórczość naturalna, skały łupkowe.

## Introduction

Natural radiation is an ubiquitous phenomenon, occurring in all parts of the planet, and nearly everything that surrounds us is radioactive [4]. Gamma measurements in Geophysical Well Logging can be divided into two types: measurements with the use of geophysical tools in boreholes and measurements on core samples, which are carried out on the surface. The results of the measurements for both methods should bring the same effect despite different environmental conditions and different layout geometry: device – rock. Radiometric measurements are always accompanied by an influence of the background, composed of: cosmic radiation, radiation from building materials, impurities in the crystal of the detector, contamination in the measurement system and the measurement method itself [1].

In case of measurements on core samples, the location of the research is important. In order to obtain the best results it is recommended to select a space with the lowest radioactive background, especially if measurements are being carried out on rocks of low radioactivity.

Measurements of the natural radioactivity of rock formations have been carried out for over half a century [11]. Initially, only the total number of detector readings were used to estimate the shaliness of the rocks examined. In the 1970s, gamma spectrometers started to be used for borehole

measurements, and on the basis of the spectrum recorded, the concentration content of individual radioactive elements began to be estimated: potassium, uranium and thorium [1]. Even currently, based on the spectrometric gamma measurements, parameters are estimated, such as: organic matter content, establishing the presence and type of clay minerals, establishing the sedimentary environment and identifying diagenetic processes in sedimentary rocks. Carrying out gamma profiling also facilitates establishing the approximate lithology of the drilled rocks [7]. In the interpretation of Well Logging, based on the radiometric measurements it is easy to draw the line between a sandstone, a carbonate rock and a shale rock, on the basis of the “total” measurements expressed in API units (American Petroleum Institute). For instance, carbonate rocks exhibit readings on the 15÷20 API level, while for shale it ranges from 75 to 150, and in some cases, the readings for highly radioactive layers indicate even up to 300 API [2]. In the case of unconventional deposits, gamma measurements are of key importance. Shale formation rocks are characterised by increased radioactive elements content. On the basis of the authigenic uranium content it is possible to make an initial estimation of the organic matter content [9] and to select core intervals for further laboratory analysis. The concentration of thorium and potassium can provide information on shaliness.

### Natural radioactivity, detection devices

Gamma radiation is electromagnetic radiation of energies from a few kilo-electron volts to many mega-electron volts. In terms of physical properties, gamma radiation and X-radiation are very similar to each other, the only difference is their place of origin. X-radiation is created with the involvement of phenomena occurring in the shell, while gamma radiation is a result of nucleus disintegration. Gamma radiation is a product of nuclear transformation and is characterised by a spectrum whose shape corresponds to the characteristic energies of individual isotopes. Knowledge of the energies of those isotopes allows for an unerring identification of radioactive elements present in the examined material [8]. In geophysical measurements, three types of particle interaction between gamma radiation and matter are significant: Compton scattering, the photoelectric effect and electron – positron pair production [6].

On the spectrum, the biggest area is generated by Compton scattering, which is an undesirable phenomenon at the later stage of concentration calculation. Total absorption peaks are of a complex origin, appearing when the total energy of the incident quantum is absorbed by the crystal. Depending on the

size of the crystal and the radiation energy, it can be caused by individual photoeffects or a series of Compton scattering ending with a photoelectric effect. Pair production does not play an important role in estimating the content of individual nuclides. In reality, the three main peaks originating from radioactive elements (K, U, Th) account for only a few percent of the counts in the channels of the total area of the spectrum [1].

Many devices of various construction and capabilities are used for radioactivity detection. In geology, devices based on scintillation detectors, are the most commonly used for the detection of radioactive elements (K, U, Th). The crystal constituting the detector can be made from various materials. NaI (Tl; sodium iodide doped with thallium) is the standard crystal due to the relatively low price and high durability. Semiconductor detectors (HPGe – high – purity germanium) are more advanced, with very high prices and expensive exploitation as the system has to work in very low temperatures. Their great advantage is very high resolution (0.2%), which contributes towards accurate qualitative analysis of radioactive elements. Unfortunately, germanium detectors have low efficiency, which results in long measurement times [12].

## Measuring equipment – calibration

A CoreLab gamma spectrometer was used to carry out the research. The measuring equipment consists of: a spectrometer, computer with software, cables, a  $^{137}\text{Cs}$  source and a set of standards.

The construction of Gamma Logger is based on a detector made of a scintillation crystal NaI(Tl),  $2' \times 2'$  in size, a photomultiplier, amplifier and a multichannel analyzer. The detector is placed in a special lead casing, limiting the influence of background activity. The shape of the casing and its mounted at the bottom wheels, allow for a comfortable placement and mobility of the device on core samples. The computer is equipped with WSG software (Well Site Gamma Logger), which allows device operation, equipment calibration, recording readings and spectra, and creating summarizing files including an indication of the depth. The set of standards includes: a  $^{137}\text{Cs}$  source, potassium standard – K (4.5%), uranium standard – U (100 ppm), thorium standard – Th (100 ppm), background measurement standard (inactive) and a “200 API” standard.

At least 30 minutes before commencing work the device needs to be connected to the power supply. The detector requires time to warm up fully and achieve a stable temperature. The first step to start the calibration is the correct spectrum setting in the appropriate energy range. To do so, the caesium source  $^{137}\text{Cs}$  is used. The manufacturer recommends that the amplification parameters should be adjusted so that the peak from caesium is present in channel 82, which corresponds to the energy of 0.662 MeV. The parameter selection hugely depends on the temperature, its sudden change will cause the peak to shift to other energy ranges – “gain drift”. The result of a peak drift is a change in the count range of the detector in the preset windows, a consequence of which are significant errors. The next step is measuring the calibration samples. The background is calibrated first with the use of the inactive standard. Subsequently, the total activity is calibrated using the 200 API standard, allowing aggregated “total” measurements

to take place. In order for the program to allow us to carry out a full spectrum measurement, the calibration needs to be completed with the use of the aforementioned standards with the appropriate concentrations for potassium, uranium and thorium. The device also enables us to use standards with different parameters [13].

Before starting work on the spectra, an energy calibration of the spectrometer is needed, consisting of assigning energy values to individual channels. The results of the measurements of the samples are used for this purpose, which enables us to obtain the following values: channel 177 corresponds to the energy from potassium isotope  $^{40}\text{K}$  – 1.46 MeV, channel 212 corresponds to the energy of 1.76 MeV originating from uranium series, while the peak from thorium series – 2.62 MeV is located in channel 315. The location of the peak from caesium ( $\text{Cs}^{137}$ ) constitutes an additional piece of information, its energy (0.662 MeV) is assigned to channel 82. A correlation graph, Figure 1, representing the calibration process can be found below.

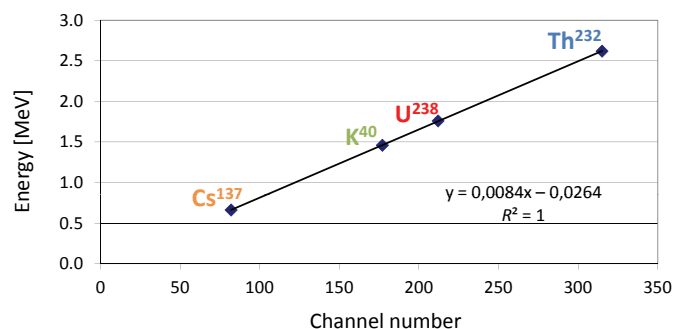


Fig. 1. A correlation graph: channels converted into energy

The energy scale obtained will be used to represent and locate spectra originating from the measurements carried out with the use of the Gamma Logger, it will also allow for a comparison with spectra from other devices which record readings on an energy scale.

## Matrix method, energy windows selection

To carry out work on measured spectra it is necessary to create a spreadsheet based on the matrix method, which is an elementary method of solving equations with multiple variables. In order to make calculations the method was applied to analyze gamma spectra emitted as a result of the radiological capture of neutrons, presented by Jacobson and Wyatt [5]. Zorski [14] is the author of the basic version of the sheet applying the matrix method. The WSG computer program allows spectrum to be projected and recorded in

a text file format, including information on the counts for individual channels.

Over the years, many theories have been created on the selection of the number and ranges of energy windows, in which impulses coming from the decay of radioactive particles are counted. The simplest way is to define three basic windows, in the areas of energies characteristic for potassium, uranium and thorium; this configuration of windows was used by IAEA (The International Atomic Energy Agency, 1976).

Unfortunately, this method loses information from the low-energy part of the spectrum. The Schlumberger company introduced a method using a significantly higher spectral range for spectrum measurements, based on 5 energy windows to include the spectrum in the range from 0.2 to 3.0 MeV [10]. P. Blum [2] divided spectra into more intervals. He isolated as many as 16 energy windows and performed an evaluation regarding the intervals in which the counts correspond to particular elements. From the entire spectrum, the best 9 matching windows were selected [1].

The matrix method allows for calculations to be made for the selected number of windows. The best solution is to make spectrum calculations for the 3-window and 9-window methods, in order to compare the results with the readings obtained directly from the device. The calculations were done on a spreadsheet created in the Microsoft Excel application, enabling a conversion to the spectrum recorded by the device, into actual contents of individual elements. Before commencing calculations, the algorithm needs to be calibrated in terms of the concentration content being determined of the elements found in the rocks. For calibration purposes, the spectra from the measurements of the standards were used.

The 9-window method covers the low-energy part of the spectrum, it also allows for its division into a higher number of intervals and for a more accurate match between the windows and the individual peaks from radioactive elements. Table 1 shows the intervals of nine windows used for calculations. The most important factor for the low-energy part of the spectrum are the peaks occurring on energies: 0.61 MeV for uranium (window no. 1), 0.86, 0.91, 0.97 MeV for thorium (window no. 3). These are peaks rising significantly above the background, therefore they carry additional information which was omitted in the 3-window method.

Table 1. Energy windows in the 9-window method

	Energy range [MeV]	
	From	To
1 – U*	0.54	0.71
2	0.72	0.85
3 – Th*	0.86	1.07
4	1.08	1.33
5 – K	1.34	1.57
6 – U	1.71	1.88
7	1.98	2.25
8	2.32	2.47
9 – Th	2.48	2.80

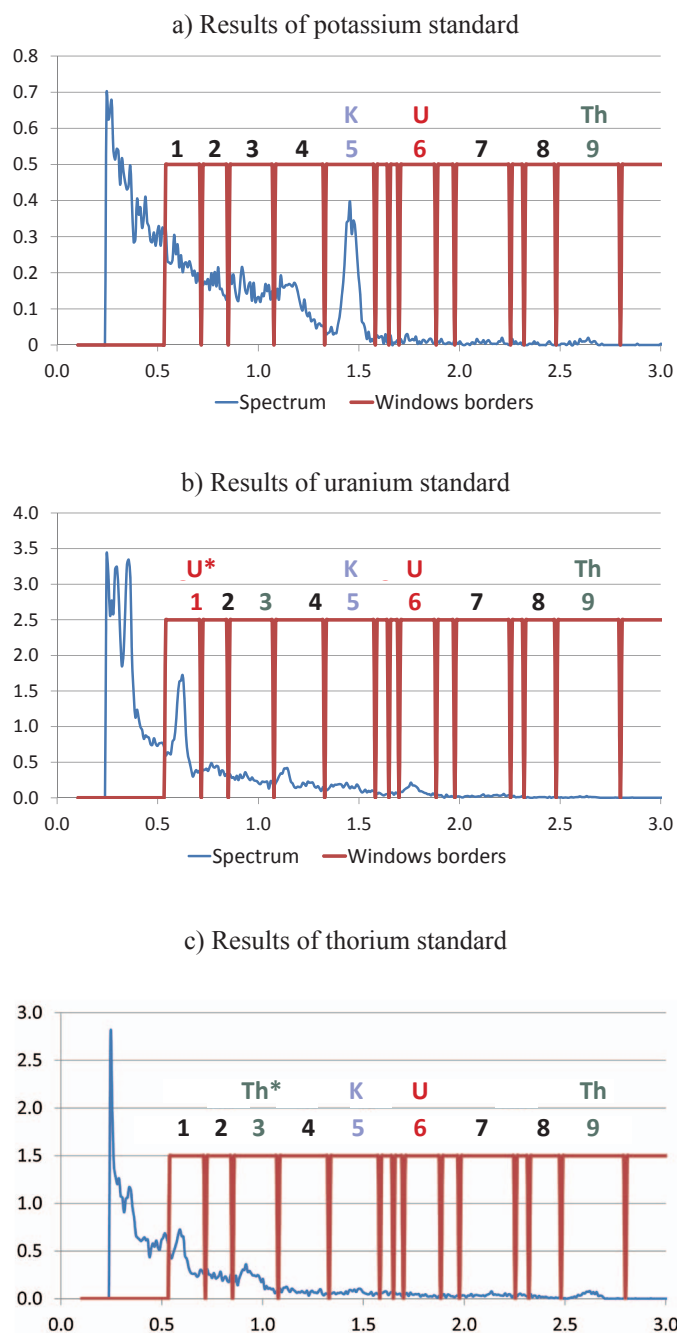


Fig. 2. 9 – energy windows displayed on the spectra of the samples measured

Energy windows borders, should match the spectrum in such a way, that the appropriate peaks are in the given windows, and the borders run in-situ minima. Figure 2 presents a comparison between the spectra from the measurements of the potassium, thorium and uranium samples. On the spectra analyzed, the borders of the following windows were marked: 5 – potassium, 6 – uranium, 9 – thorium. Additional “strong” peaks from uranium and thorium were indicated on the graphs as U\*, Th\*.

Measurements on shale cores

The results were divided into 3 groups: results obtained directly from the device (the 3-window method), results obtained with the use of the matrix method with 3 energy windows and with 9 energy windows. The purpose of the application of the 9-window method, was to achieve a reduction of errors, without extending the measurement time. The 9-window method, should increase the accuracy of the results obtained, however, increasing the number of windows does not only increase the number of counts, but also the impact of the background.

The research material were shale cores; shale being formations rich in clay minerals and organic matter, therefore it was certain that the results would indicate higher readings. The research was conducted in a laboratory and a core repository. To confirm the analyses, a stationary MAZAR spectrometer was used, which is characterised by a high accuracy. The measurement time on the laboratory device was set to 6 hours. Circa 150 g of crushed and divided material was examined.

To carry out the measurements in the laboratory, five points of measurement were chosen on selected parts of the core. Each of the points was measured five times in order to estimate the measurement error. An analysis conducted with the use of the MAZAR device was performed only once for each sample.

Table 2 shows the results obtained from the MAZAR device and Gamma Logger. The first set of results marked in yellow is standard measurements. Orange indicates a measurement series calculated with the 3-window matrix method, and red indicates a series calculated with the 9-window method. The columns marked with „STAT”: average, standard deviation, measurement error [%].

An analysis of the results presented in Table 2 will be considered in regard to the accuracy of the measurements for one measurement point and in regard to matching the result from the mobile device to the laboratory equipment.

Figure 3 shows the results for three measurement points (Core 1, Core 2, Core 3) from Table 2. Individual elements are

Table 2. Comparative results: MAZAR – Gamma Logger equipment

MAZAR – 6 h				Gamma Logger (CoreLab) – measurement time: 5 min																				
				Gamma Logger						Gamma Logger – 3 windows						Gamma Logger – 9 windows								
Core	K	U	Th	K	STAT	U	STAT	Th	STAT	K	STAT	U	STAT	Th	STAT	K	STAT	U	STAT	Th	STAT			
Core 1	3.29	16.8	11.34	0.94		10.43		10.29		1.68		16.76		16.1		2.54		9.28		15.17				
				1.49	1.51	8.12	8.53	0.53	5.54	2.56	2.32	8.56	11.57	15.18	14.27	2.33	2.50	9.61	9.61	16.33	14.61			
				1.92	0.42	10.54	2.12	0.18	5.05	2.29	0.39	10.63	3.07	18.39	4.06	2.99	0.29	7.25	2.00	12.42	3.28			
				1.91	27.50	5.35	24.87	6.16	91.06	2.67	16.65	10.75	26.53	7.57	28.48	2.30	11.47	12.78	20.78	10.38	22.45			
				1.31		8.23		10.55		2.40		11.17		14.11		2.36		9.13		18.74				
Core 2	2.58	19.35	8.59	1.46		10.37		8.46		2.47		13.67		12.1		2.53		11.13		15.85				
				1.55	1.60	12.41	10.68	0.16	3.65	2.36	1.97	12.94	13.72	18.61	15.00	2.34	2.48	12.85	11.17	13.79	14.96			
				1.89	1.00	7.77	3.57	7.79	4.14	1.53	0.52	18.36	3.85	12.65	4.75	2.22	0.41	12.61	1.95	13.57	3.01			
				0.16	62.44	15.81	33.44	1.72	113.37	1.50	26.55	15.68	28.03	21.38	31.67	2.14	16.49	11.28	17.43	19.73	20.14			
				2.95		7.05		0.13		3.32		7.96		10.25		3.16		7.97		11.88				
Core 3	3.44	11.09	14.47	0.42		13.35		0.16		2.43		8.43		16.97		2.38		11.8		11.82				
				1.29	1.25	12.76	11.97	1.31	0.48	2.64	2.57	9.90	8.72	15.90	18.77	2.98	2.68	8.09	9.56	13.76	13.68			
				2.06	0.68	9.21	1.76	0.39	0.47	3.02	0.42	6.65	6.55	18.66	9.07	2.90	0.36	7.75	1.66	15.28	4.14			
				0.75	54.07	13.29	14.74	0.38	97.97	1.93	16.42	18.39	75.06	8.79	48.33	2.93	13.48	10.01	17.36	8.18	30.24			
				1.73		11.22		0.18		2.85		0.23		33.54		2.20		10.16		19.35				
Core 4	2.23	0.58	9.38	0.10		5.06		0.13		1.58		5.22		15.39		1.66		4.10		12.43				
				0.18	0.27	4.86	3.55	0.19	0.16	1.90	1.44	3.45	5.87	11.45	14.25	1.93	1.91	2.69	2.35	11.68	13.15			
				0.32	0.22	2.55	2.17	0.19	0.04	1.44	0.45	4.30	2.53	18.94	3.78	2.03	0.15	1.19	1.14	14.00	1.21			
				0.11	81.40	5.10	61.00	0.20	24.99	0.70	31.01	9.93	43.07	16.01	26.53	2.00	7.66	1.56	48.37	12.92	9.23			
				0.62		0.18		0.11		1.56		6.44		9.46		1.92		2.21		14.71				
Core 5	1.67	1.68	5.04	2.61		0.15		0.13		2.02		8.57		8.44		2.48		2.31		10.95				
				1.90	1.59	0.13	1.61	0.13	0.14	2.09	1.91	5.22	6.52	13.13	13.13	2.45	2.38	1.55	1.76	12.45	13.52			
				2.24	1.00	0.19	3.23	0.16	0.02	2.19	0.34	4.55	1.62	14.19	4.86	2.41	0.15	1.38	0.59	14.40	1.83			
				1.05	62.91	0.20	200.35	0.13	11.57	1.92	17.74	7.03	24.88	9.25	37.03	2.44	6.39	1.10	33.68	14.12	13.57			
				0.13		7.38		0.16		1.33		7.21		20.64		2.11		2.45		15.66				

presented on separate graphs. Each of the graphs is divided into three segments, and each segment contains a comparison of the three measurement methods. From the left side of the graph, statistics for the results obtained directly from the device (GL), for the 3-window method (GL\_3 windows) and for the 9-window method (GL\_9 windows) are shown respectively.

An analysis of the graphs facilitates a fast evaluation of the accuracy of the three methods in regard to the three elements examined. The result graph for potassium is the easiest to interpret. The error in the results obtained directly from the device is the largest, and the dispersion is relatively high; the other methods produced a lesser range of errors and more proximate results. An analysis of the uranium also indicates

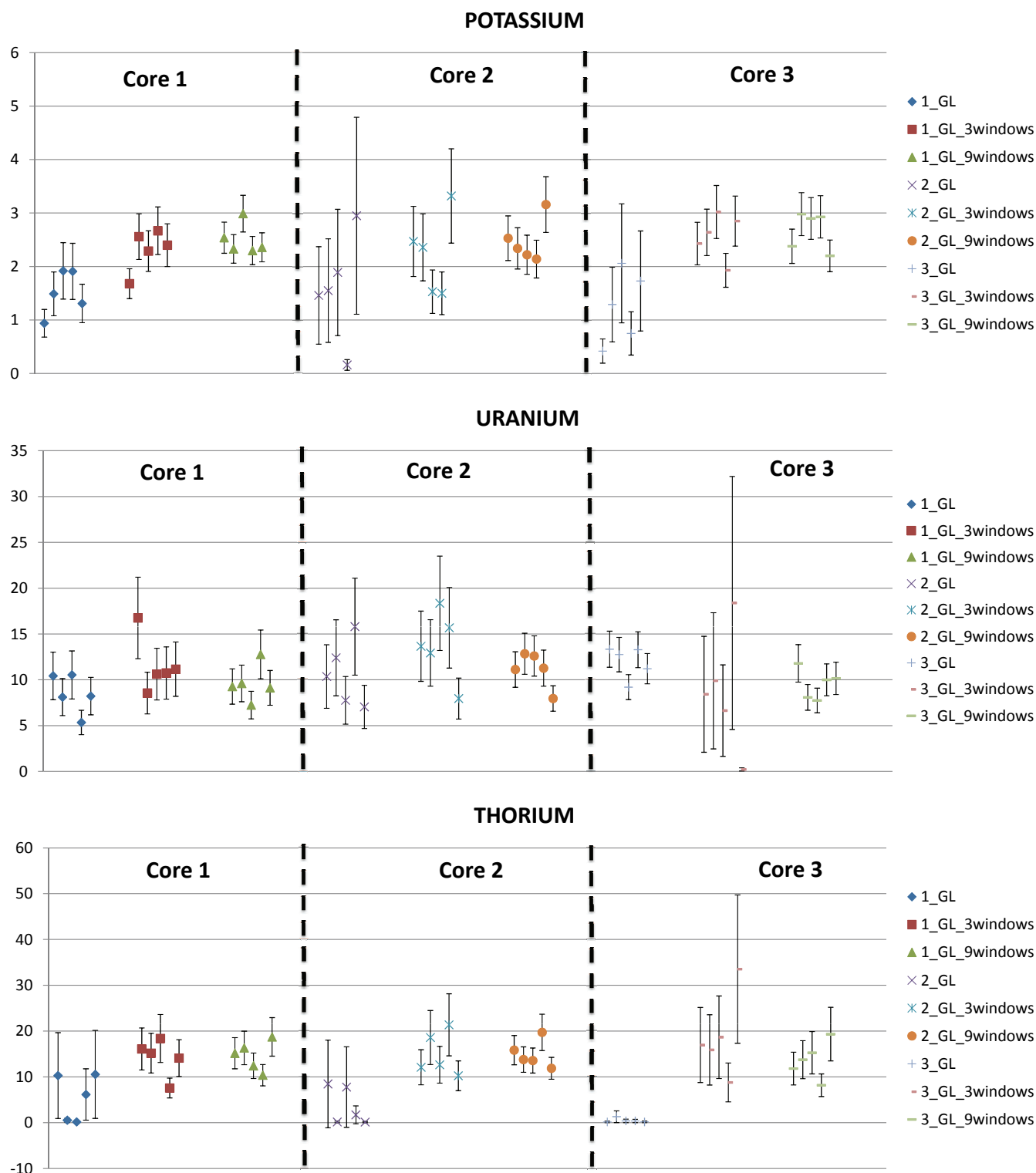


Fig. 3. The statistics for the results from the Gamma Logger device, potassium, uranium and thorium in regard to three measurement points: Core 1, Core 2, Core 3, from Table 2

an improvement with the subsequent method, only the Core 3 measurement demonstrates a slightly larger error for the matrix methods. The statistics for thorium improved significantly even in the case of the Core 3, with one value being significantly different from the others. Due to the variable range for one measurement it is not visible on the graph, and the values can be seen on the attached Table 2. The five-minute measurement time for this type of detector is short, therefore the cause for the inaccuracies could be statistical fluctuations, whose influence is quite high in the case of 5 repetitions.

In order to compare the results and evaluate which of them is closest to the actual concentration level, additional graphs were created to show average values (Figure 4). These graphs show all measurement points and a comparison of the 4 analyses.

Figure 4. shows the results of a comparative analysis. The values measured with the MAZAR devices are treated as reference. Graph a) shows the accuracy of measurement for potassium using all of the methods. The results from the 9-window method are closest to the reference measurement values for samples 1 to 4. An analysis of graph b) which includes the values for uranium shows that the 9-window method for samples 1 to 3 was less efficient than the 3-window method, while for samples 4 and 5 it was more accurate. Graph c) showing the data for thorium demonstrates that, the results imported directly from the device are significantly lower than the actual values. The best result calculated with the use of the 9-window method was obtained in the case of the sample with the highest thorium content (Core 3). An overall analysis of the graphs indicates the level of underrepresentation of the content of radioactive elements by the Gamma Logger device and its software. This may be caused by a difference in the geometry and in the content of radioactive elements in the standards.

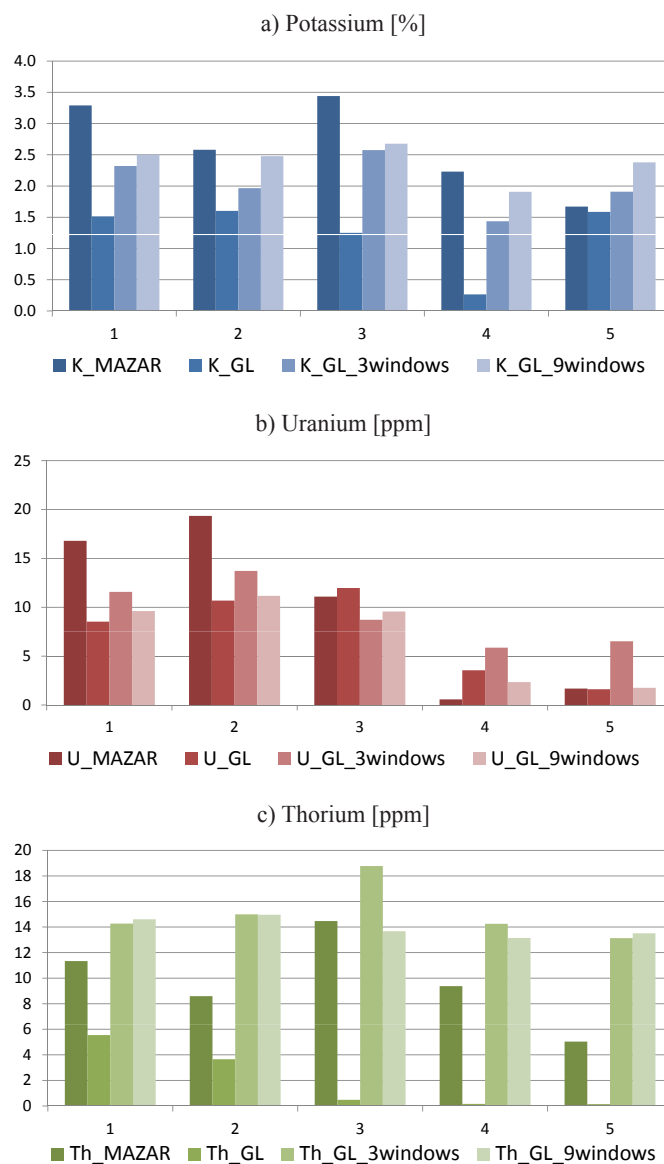


Fig. 4. A comparison between the results from the mobile device Gamma Logger and laboratory analyses, MAZAR

### Field measurements

In order to conduct a device test, field measurements were taken in the core repository. The measurement area was characterised by a lower background than the laboratory background. A one-metre long core sample characterised by an increased radioactive elements content was examined. A full calibration of the spectrometer was carried out, and the spectra registered during this process were recorded in order to be used to calibrate the spreadsheet at a later stage. The measurement step was 10 cm, and the measurements were carried out in series of five for each point. The results were calculated with the use of the 3-window and 9-window matrix method and summarised in Table 3.

An overall evaluation of the measurements taken indicates that again the lowest errors were registered for the

9-window method. The measurement error for potassium is also worth noticing, as it is smaller than in the case of the measurements conducted in an environment with a higher background (Table 2).

The measurements on the one-metre long core sample were carried out in order to prepare graphs of spectrometric gamma profiling for various methods and to compare them. The results are presented in three different graphs (Figure 5), separately for potassium, uranium and thorium. Figure 5 shows the results of the calculations summarised in Table 3. An analysis of the graph indicates that the values increase with each subsequent method. The graph for uranium is an exception, in this case the 9-window method returned lower values than the 3-window method. The analysis of the profiling displayed,

Table 3. Results of field analyses conducted with the Gamma Logger spectrometer

Gamma Logger (CoreLab) – measurement time: 5 min																		
Gamma Logger						Gamma Logger – 3 windows						Gamma Logger – 9 windows						
	K	STAT	U	STAT	Th	STAT	K	STAT	U	STAT	Th	STAT	K	STAT	U	STAT	Th	STAT
1	2.24		1.53		0.16		2.88		5.16		8.75		3.14		3.24		8.01	
	1.73	1.69	0.76	1.21	5.64	3.17	2.88	2.57	4.09	6.88	7.77	7.49	3.25	3.04	2.25	2.67	8.70	10.23
	1.05	0.43	0.38	0.61	9.77	4.39	1.84	0.47	9.07	2.83	12.7	3.62	2.54	0.30	1.97	0.90	17.36	4.05
	1.64	25.21	1.56	50.17	0.13	138.48	2.91	18.33	5.43	41.05	4.76	48.38	3.26	9.81	1.90	33.94	9.49	39.57
	1.79		1.80		0.15		2.35		10.66		3.46		2.99		3.97		7.60	
2	2.47		1.74		0.11		3.13		4.77		7.44		3.22		3.31		9.64	
	2.11	2.04	0.21	1.03	1.25	5.67	2.40	2.54	8.06	6.87	10.72	10.24	3.01	2.98	2.26	2.97	11.17	11.75
	2.36	0.44	2.07	0.88	0.18	9.94	2.15	0.37	9.99	2.48	13.71	2.36	2.97	0.16	2.41	0.70	12.62	2.07
	1.88	21.69	1.01	85.70	3.52	175.38	2.38	14.66	7.60	36.14	8.82	23.00	2.93	5.22	3.99	23.70	10.44	17.60
	1.36		0.11		23.27		2.63		3.94		10.53		2.79		2.88		14.89	
3	1.85		4.94		0.20		3.11		5.87		1.75		3.53		3.04		5.07	
	1.35	1.84	2.53	2.21	9.31	6.30	2.54	2.72	6.61	6.09	9.29	8.83	2.92	3.16	3.50	2.74	12.8	11.07
	1.75	0.43	0.69	1.85	9.66	4.16	2.66	0.23	3.84	2.07	13.79	4.68	3.08	0.24	1.21	0.88	15.08	3.86
	1.72	23.16	2.61	83.90	3.76	66.00	2.59	8.35	5.21	33.97	12.02	53.00	3.03	7.45	2.98	32.23	12.71	34.92
	2.52		0.28		8.57		2.69		8.68		7.28		3.22		2.97		9.67	
4	1.77		4.04		0.19		2.69		5.63		9.82		2.81		4.81		9.30	
	2.91	2.16	0.17	2.08	3.37	1.37	2.94	2.84	6.11	4.61	6.14	11.33	3.36	3.01	2.81	3.47	9.65	11.70
	1.97	0.45	1.46	1.58	2.02	1.36	2.99	0.13	1.81	1.82	18.49	4.55	2.92	0.24	1.98	1.16	16.98	3.19
	2.21	20.73	3.36	75.95	0.13	99.67	2.74	4.49	5.77	39.52	10.01	40.20	3.15	7.90	3.29	33.60	10.17	27.25
	1.94		1.38		1.12		2.86		3.72		12.19		2.82		4.44		12.41	
5	1.14		4.93		6.91		2.62		4.81		14.22		2.83		3.23		14.87	
	1.5	1.54	2.89	4.21	0.66	2.19	2.32	2.57	9.16	7.24	4.64	9.67	2.73	2.91	6.02	4.16	8.85	11.36
	1.95	0.30	3.61	0.92	1.97	2.70	2.10	0.36	11.25	2.89	9.53	3.63	2.98	0.14	3.84	1.08	11.07	2.46
	1.42	19.66	4.67	21.76	0.91	123.48	2.99	14.04	4.58	39.99	8.20	37.49	3.08	4.64	3.69	25.95	9.39	21.65
	1.69		4.93		0.49		2.81		6.38		11.77		2.93		4.03		12.63	
6	1.83		3.40		8.82		2.77		7.03		9.41		3.17		3.29		11.04	
	1.96	2.38	1.76	2.15	7.92	5.32	2.40	2.81	8.43	6.77	9.28	9.42	3.09	3.19	3.28	3.37	12.05	11.27
	2.92	0.53	0.16	1.29	7.57	3.89	3.07	0.35	2.43	2.52	14.1	3.25	3.05	0.23	3.07	0.43	14.58	2.79
	2.97	22.47	2.26	60.25	0.20	73.10	3.24	12.40	7.32	37.26	4.91	34.51	3.59	7.12	3.11	12.70	6.89	24.73
	2.22		3.15		2.11		2.56		8.64		9.39		3.06		4.12		11.78	
7	1.56		2.05		0.86		2.54		6.39		10.12		2.96		3.25		12.47	
	2.45	1.97	6.02	2.94	0.20	0.50	2.60	2.66	9.59	7.07	8.12	8.49	3.61	3.07	3.00	3.86	5.40	9.57
	2.19	0.44	1.13	1.85	0.13	0.39	2.68	0.22	5.06	1.75	11.17	2.11	2.58	0.42	5.24	1.05	12.14	3.02
	1.44	22.54	2.62	62.95	0.99	78.25	2.47	8.21	7.99	24.72	6.58	24.84	2.82	13.55	4.75	27.19	10.19	31.60
	2.22		2.86		0.34		3.03		6.34		6.45		3.36		3.08		7.63	
8	2.71		0.76		0.23		3.37		2.41		11.22		3.25		3.16		10.89	
	2.3	2.41	0.16	2.16	8.09	2.70	3.27	3.12	1.43	3.79	11.91	10.10	3.12	3.19	0.96	2.95	15.10	11.13
	1.75	0.40	4.35	2.36	1.20	3.35	2.48	0.41	6.52	1.99	11.16	2.55	3.01	0.14	3.23	1.18	12.52	3.25
	2.66	16.67	0.44	109.27	3.80	124.01	2.95	13.26	4.74	52.55	10.59	25.27	3.20	4.25	3.30	39.96	10.96	29.17
	2.62		5.08		0.19		3.52		3.83		5.61		3.37		4.12		6.19	
9	1.51		3.24		5.97		2.61		2.37		20.98		2.62		3.65		16.43	
	2.2	1.76	3.32	3.84	0.95	3.21	2.78	2.80	7.44	4.71	8.01	12.37	3.11	2.99	4.74	3.89	8.73	11.63
	1.42	0.32	4.95	0.91	0.45	3.28	2.72	0.22	4.36	2.52	11.2	5.39	2.89	0.24	4.10	0.67	10.51	2.94
	1.96	18.24	2.99	23.74	1.18	102.02	3.17	7.71	2.21	53.51	13.74	43.57	3.23	8.11	2.92	17.19	12.12	25.27
	1.72		4.70		7.51		2.72		7.19		7.92		3.12		4.04		10.36	
10	2.55		0.13		1.26		3.07		1.97		10.87		2.72		3.24		12.4	
	1.33	1.68	0.44	2.87	3.70	1.10	2.44	2.69	4.42	6.22	11.89	9.60	2.67	2.79	2.52	3.94	15.8	11.13
	1.00	0.84	7.08	3.31	0.20	1.53	1.72	0.27	12.39	3.92	4.62	3.73	2.62	0.17	6.76	1.73	5.63	4.03
	2.62	50.30	0.87	115.43	0.22	138.84	2.67	10.18	5.18	62.92	13.70	38.91	3.00	5.93	2.78	44.00	13.27	36.17
	0.89		5.81		0.12		2.56		7.16		6.90		2.92		4.38		8.56	

also allows, for an assessment of the discrepancies between the points measured subsequently. The 9-window matrix method

is characterised by the lowest variability of the results for the subsequent measurement points and the deviation is reduced.

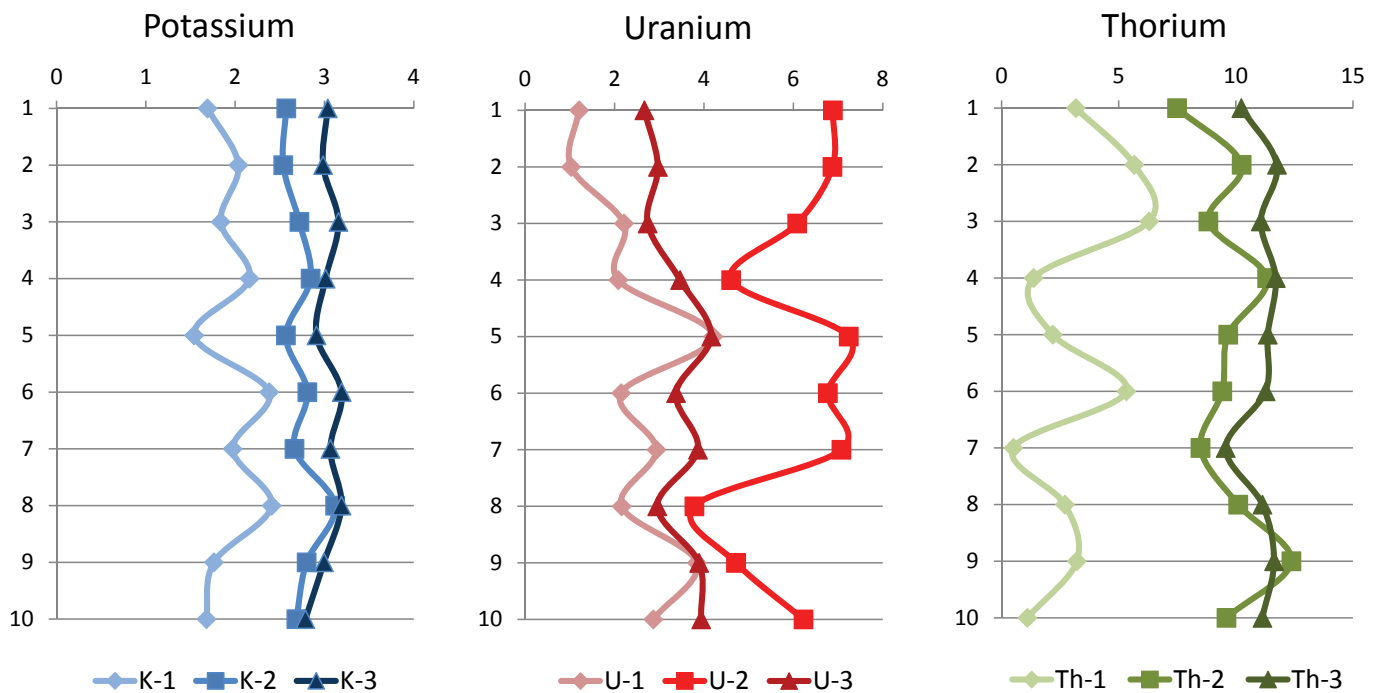


Fig. 5. Spectrometric gamma profiling for a one-meter long core sample.  
 1 – result from Gamma Logger, 2 – result from the 3-window method, 3 – result from the 9-window method

### Conclusions

Conducting research on shale formation core samples facilitated an examination of the influence of statistical fluctuation on the results obtained. The analyses were conducted with the use of the Gamma Logger measuring equipment based on the scintillation detector NaI(Tl) 2 × 2'. In order to improve the accuracy of the results, a calculation algorithm was drawn up, based on the matrix method using 9 energy windows, which include the low-energy part of the spectrum. The calculations carried out on the exported spectra allowed for a current overview of the results and the location of the borders for individual windows. The user has full control over setting the energy windows in suitable positions, which can significantly improve the adjustment of the borders of the intervals in case of a drift.

The measurements took place in a laboratory as well as in the core repository. The results obtained from direct measurements and through the matrix methods (3 and 9 windows) were presented in table form and as graphs. The first phase of the research conducted in the laboratory provided

a comparison between the results and the MAZAR equipment, which resulted in reference results being established. An analysis of the data showed that the 9-window matrix method decreased the influence of statistical fluctuations on the result and the measurement error calculated. The accuracy of the measurements in comparison with the MAZAR analyses also improved in most cases. The second series of measurements conducted in the field were aimed at creating a spectrometric gamma logging on a shale rock core sample. The results obtained directly from the device and from the matrix methods were compared. Also in this case a significant improvement in the measurement statistics was noticeable.

The algorithm based on the publication of Jacobson and Wyatt, prepared as spreadsheet by Zorski is a universal program, which can be used for the purpose of working with spectra originating from other devices, or with different parameters of calibration standards. The only requirement is a spectrum from a detection device recorded in a numerical form.

Please cite as: Nafta-Gaz 2015, no. 6, pp. 390–399

Article contributed to the Editor 19.01.2015. Approved for publication 25.03.2015.

The publication was based on the statutory project of INiG – PIB, Kraków: *Ocena dokładności wyznaczania koncentracji pierwiastków promieniotwórczych na rdzeniach skał łupkowych* – order no.: 33/SW/2014.

## Bibliography

- [1] Blum P., Rabaute A., Gaudon P., James F. Allan: *Analysis of natural gamma-ray spectra obtained from sediment cores with the shipboard scintillation detector of the ocean drilling program: example from leg 1561*. Shipley T. H., Ogawa Y., Blum P., Bahr J. M. (Eds.), Proceedings of the Ocean Drilling Program, Scientific Results 1997, vol. 156.
- [2] Blum P.: *Natural gamma radiation Ocean Drilling Program*. PP Handbook, November 1997, pp. 5–15.
- [3] Bolesta F., Galazka A.: *Profilowanie gamma – przeliczanie jednostek*. Nafta-Gaz 2014, no. 8, pp. 493–501.
- [4] Hendriks P. H. G. M., Limburg J., de Meijer R. J.: *Full-spectrum analysis of natural g-ray spectra*. Journal of Environmental Radioactivity 2001, 53, pp. 365–380.
- [5] Jacobson L. A., Wyatt D. F.: *The elemental Yields and Complex Lithology Analysis From the Pulsed Spectral Gamma Log*. The Log Analyst – A journal of formation evaluation and reservoir description. Jan.-Feb. 1996, pp. 50–64.
- [6] Jarzyna J., Bala M., Zorski T.: *Metody geofizyki otworowej – pomiary i interpretacja*. Wydawnictwa AGH, Kraków 1997.
- [7] Kowalska S., Lewandowska A., Buniak A.: *Przyczyny powstawania anomalnych wskazan profilowania gamma (sPG) w skałach czerwonego spagowca z rejonu wyniesienia wolsztyńskiego*. Nafta-Gaz 2010, no. 6, pp. 425–440.
- [8] Lisieski W.: *Praktyczna spektrometria promieniowania gamma w badaniach technicznych*. Nowa Technika, zeszyt 70, Wydawnictwa Naukowo-Techniczne, Warszawa 1967.
- [9] Lüning S., Kolonic S.: *Uranium spectral gamma-ray response as a proxy for organic richness in black shales: applicability and limitations*. Journal of Petroleum Geology, April 2003, vol. 26 (2), pp. 153–174.
- [10] Serra O., Baldwin J., Quirein J.: *Theory, interpretation and practical applications of natural gamma ray spectroscopy*. Transactions of the SPWLA 21<sup>st</sup> Annual Logging Symposium 1980, 27:Q1–Q30.
- [11] Serra O.: *Fundamentals of Well-Log Interpretation (vol. 1): The Acquisition of Logging Data*. Developments in Petroleum Science, 15A, Amsterdam (Elsevier), 1984.
- [12] Dobrzyński L.: Website: [http://ncbj.edu.pl/zasoby/wyklady/ld\\_stud\\_podypl/04.deteckja.pdf](http://ncbj.edu.pl/zasoby/wyklady/ld_stud_podypl/04.deteckja.pdf) (access: 2014).
- [13] Zalewska J., Antosz K., Cebulski D.: *Badania rozkładu naturalnej promieniotwórczości rdzeni wiertniczych przy wykorzystaniu wyników analiz rejestracji urządzeniem Gamma Logger, pomiarów otworowych geofizyki wiertniczej oraz pomiarów laboratoryjnych*. Praca statutowa, Kraków 2012, Nr arch.: DK-4100-59/12, Zlec. wew. INiG 158/0059/12.
- [14] Zorski T.: *Arkusze kalkulacyjne do przybliżonej symulacji widm naturalnego promieniowania gamma i ich dekompozycji*. Niepublikowane materiały dydaktyczne, 2012.



Rafał SKUPIO  
M.Sc., Eng., Engineering Support Specialist,  
Department of Well Logging  
Oil and Gas Institute – National Research Institute  
ul. Lubicz 25A  
31-503 Kraków  
E-mail: [rafal.skupio@inig.pl](mailto:rafal.skupio@inig.pl)